Nuclear Radiation-Induced Atmospheric Air Breakdown in a Spark Gap

Shaolin Liao, Nachappa Gopalsami, *Senior Member, IEEE*, Eugene R. Koehl, Thomas W. Elmer, II, *Member, IEEE*, Alexander Heifetz, Hual-Te Chien, and Apostolos C. Raptis, *Life Member, IEEE*

***Abstract*—We have investigated the effect of pre-ionization by a radioactive ^{137}Cs γ-ray source on the atmospheric air breakdown conditions in a high-voltage spark gap. A standoff millimeter-wave (mmW) system was used to monitor the breakdown properties. A decrease in breakdown threshold was observed with an increase of radiation dose. We attribute this to a space charge-controlled electron diffusion process in a cloud of radiation-induced ion species of both polarities. The space charge-dependent diffusion coefficient was determined from the measurement data. In addition, we found that the breakdown process shows random spikes with Poisson–like statistical feature. These findings portend the feasibility of remote detection of nuclear radiation using high-power mmWs.**

***Index Terms*—Air breakdown, breakdown voltage, millimeter wave (mmW), nuclear radiation, spark gap.**

I. Introduction

ATMOSPHERIC AIR breakdown has been of great interest in plasma physics [1], and its potential application to remote detection of nuclear radiation-induced ionized air has been explored recently [2]. Although the spark gap breakdown has been known [3] for plasma generation, the physics of breakdown parameters is not well understood in the presence of nuclear radiation, particularly at atmospheric pressure. In this paper, we present an analysis of the nuclear radiation-induced air breakdown process in a dc spark gap and its detection with a standoff millimeter-wave (mmW) system. The purpose of our investigation is twofold: 1) demonstrate feasibility of high-power mmW remote detection of nuclear radiation-induced ionized air from its equivalent dc air breakdown investigation and 2) shed light on the fundamental physics governing the nuclear radiation-induced air breakdown process.

II. Theoretical Background

A. DC Spark Gap and High-Power Microwave Breakdown

dc spark gap breakdown can be categorized into two types [4]: the Townsend process at low pressure (p)—spark gap separation (d) product, i.e., the pd value; and the streamer process at high pd value. The Townsend type is an electron avalanche process that involves both primary ionized electrons in the air and the secondary electrons emitted at the cathode due to impact of the positive ions [5], [6]. The breakdown voltage can be obtained by solving the generalized Townsend equation [7]. A streamer is a filament-like structure due to strong electric field around the rapidly advancing and highly concentrated avalanche front [8], [9].

The high-power microwave air breakdown can be explained in terms of the effective electric field strength, i.e., $E_{eff} = E_{rms}/\sqrt{1+(\omega/\nu_c)^2}$, where E_{rms} is the root-mean-square electric field and ω and ν_c are the electromagnetic circular frequency and electron collision frequency in the air, respectively. High-power microwave experiments have also been studied in various frequency bands and resonant cavities [10].

In both cases, breakdown electric field is obtained when the electric field-dependent ionization rate ν_i equals the attachment loss rate ν_a plus the diffusion loss rate ν_d,

$$\nu_i(E_b) = \nu_a(E_b) + \nu_d(E_b) \sim \nu_a(E_b) - \frac{D}{\Lambda_{eff}^2} \tag{1}$$

where E_b is the breakdown dc or effective electric field strength and D and Λ_{eff} are the diffusion coefficient and effective diffusion length, respectively. When $\nu_i \ll \nu_d$, (1) gives,

$$D \sim \nu_i(E_b)\Lambda_{eff}^2. \tag{2}$$

B. Preionization and Afterglow Effect

Microwave breakdown under various background ionization concentrations ranging from $10^6 - 10^9$ cm^{-3} has been tested [11] with a microwave cavity using Neon gas at pressures up to 100 torr. It has been found that the breakdown field strength could be reduced by more than 10% in the presence of pre-ionization. The authors related such remarkable observation to the transition from the free electron diffusion to the ambipolar diffusion, which means the diffusion coefficient is also a function of ion density n_i, $D(n_i)$; however, its detailed form has not been obtained. The laser pre-ionization effect for an atmospheric spark gap based on resonance enhanced multi-photon ionization mechanism has also been investigated recently [12], where a reduction of breakdown voltage up to 50% has been achieved. However, the laser induced pre-ionization is along the path of the laser instead of the whole space in the spark gap.

The afterglow in both dc spark gap and microwave air breakdown has a similar transition from space charge-controlled

Manuscript received October 25, 2011; revised January 17, 2012; accepted January 29, 2012. Date of publication March 2, 2012; date of current version April 11, 2012. This work was supported by the Defense Threat Reduction Agency under the U.S. Department of Energy Contract No. DE-AC02-06CH11357.

The authors are with the Nuclear Engineering Division, Argonne National Laboratory, Argonne, IL 60439 USA (e-mail: sliao@anl.gov; goplasami@anl.gov; dick.koehl@anl.gov; elmer@anl.gov; aheifetz@anl.gov; htchien@anl.gov; raptis@anl.gov).

Color versions of one or more of the figures in this paper are available online at http://ieeexplore.ieee.org.

Digital Object Identifier 10.1109/TPS.2012.2187343

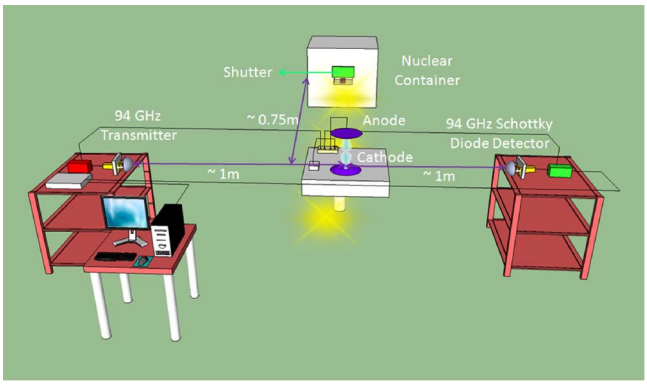

Fig. 1. Schematic diagram of nuclear radiation-induced air breakdown in a spark gap between hemispherical electrodes.

diffusion to free electron diffusion for various gas species [13]–[16]. It has been shown that the electron diffusion could be noticeably modified by the space charge effect.

C. Nuclear Radiation-Induced Air Breakdown

In the case of nuclear radiation-induced atmospheric air breakdown process, the background air contains many molecular species including dust/aerosols, along with the production of free electrons, positive, and negative ions. These variables affect the overall dependency of the radiation dose $\Re$ on the breakdown electric field, E_b, which is a key parameter for assessing feasibility of remote detection of nuclear radiation by high-power mmWs.

III. Experimental Description

As a first step toward establishing the feasibility of remote detection of nuclear radiation-induced air breakdown with high-power mmWs, we used an air gap between two electrodes maintained at high voltage to simulate the focal plane of a high-power beam. Charges in air due to nuclear radiation are accelerated by the high voltage to produce avalanche breakdown, which can be sensed remotely. Fig. 1 is a schematic diagram of experimental setup showing a dc spark gap which is irradiated by a ^{137}Cs γ source; a standoff mmW transmitter and detector system at 94 GHz are used to measure the breakdown-induced transmittance changes. The dc spark gap consists of two hemispherical electrodes, separated by a distance, $d = 0.635$ mm, giving a pd value of ~48.26 torr-cm. One of its electrodes is grounded and the other is connected to a high-voltage dc power supply (Bertan Series 225), which is controlled by a wave form generator to produce a desired high-voltage sweeping function. A triangular sweep was used to generate 0 to 4 kV within a 30-s period, as shown in Fig. 2.

A nominal 20-Ci ^{137}Cs source is used as the initial electron seed source to induce the air breakdown process. Gamma rays are emitted by radioactive ^{137}Cs source in the following two-step reaction:

1) Beta decay of ^{137}Cs($T_{1/2} = 30.0$ y)

$$^{137}_{55}\mathrm{Cs} \rightarrow {}^{137m}_{56}\mathrm{Ba} + \beta^- + \overline{\nu}$$

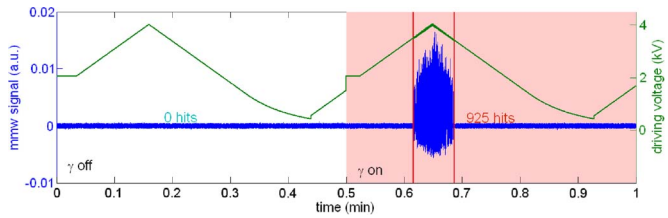

Fig. 2. Triangular sweep of dc power supply from 0 to 4 kV over a 30 s period and the corresponding mmW signal without (unshaded) and with (shaded) γ-ray radiation.

2) Gamma decay of metastable ^{137m}Ba($T_{1/2} = 2.552$ min)

$$^{137m}_{55}\mathrm{Ba} \rightarrow {}^{137}_{56}\mathrm{Ba} + \gamma.$$

The primary gamma photons with energy $E_\gamma = 661.6$ keV are produced with frequency $f = 89.78\%$. Because of much smaller half-life, ^{137}Ba daughter is in secular equilibrium with its parent ^{137}Cs isotope. Thus, ^{137}Cs source with activity $A = 20$ Ci emits $N_\gamma = 6.64 \times 10^{11}$ photons per second. Using the tabulated value of linear interaction coefficient for photons with $E = 600$ keV, the mean free path in air is $\overline{x} = 103.2$ m. The radiation facility consists of ^{137}Cs material (CIS-CS-210 type capsule) of 20 Ci strength housed in a sealed housing. The source is raised up with pneumatic control to a test position that has a rectangular opening (horn) with a cone angle of 45°. Lead plates are pneumatically inserted into the aperture to attenuate γ radiation from 0 to 99.96%. The distance from the Cs source to the spark gap is ~0.75 m.

A standoff mmW transmitter/receiver system at 94 GHz was set up to monitor the signal change due to the air breakdown. The transmitter consists of a mechanically tuned Gunn diode oscillator (Millitech model GDM-10 with ~15-dBm CW power) attached to a standard gain horn antenna that is coupled to a focusing lens of 8.9-cm diameter; the receiver consists of an identical horn antenna and lens pair attached to a Schottky barrier diode (Millitech DET-10) and a low noise amplifier. The transmitter and receiver are located on opposite sides of the γ ray beam with a ~2 m separation between them, and aligned along the centerline of the spark gap. The data were collected at 20 KS/s with a 24-bit DAQ board (National Instruments USB-4431) connected by a USB cable to a laptop. The instrument control and data collection were carried out by LabVIEW running on a laptop computer from outside the radiation controlled area.

IV. Experimental Results and Discussion

The high-voltage dc power supply was controlled by a function generator that generated a triangular sweep, achieving a voltage range from 0 to 4 kV within a 30-s period. A typical gap voltage and the corresponding mmW signal without and with full exposure of the spark gap to the ^{137}Cs source are shown in Fig. 2. It clearly shows that the air breakdown occurs only when 1) the air gap is exposed to gamma-ray radiation and 2) the applied voltage exceeds the air breakdown voltage, which corresponds to an electric field of about 35 kV/cm.

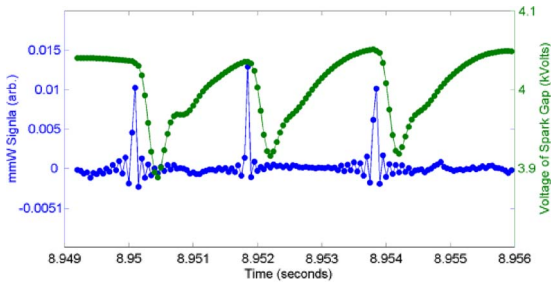

Fig. 3. Three typical spikes are shown in both mmW signal and spark gap voltage traces: the lower dotted line is the mmW signal, and the upper dotted line is the spark gap voltage; the ~ 300 μs time delay between the peak and the trough is due to the 90° phase delay of the high-voltage circuit.

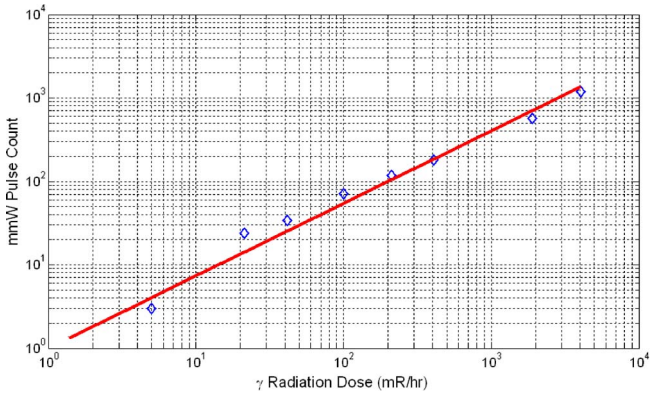

Fig. 4. mmW pulse counts as a function of γ radiation dose.

Upon further examination (zoomed in), there exists a random sequence of spikes in both mmW and gap voltage traces. Fig. 3 shows three typical spikes: the mmW spike is synchronized to the onset of spark gap current; the spark current also affects the high-voltage readout signal, which is 90° phase delayed with respect to the current of the mmW signal, hence the gap voltage trace reaches its minimum ~ 300 μs after the mmW signal peak.

By counting the mmW spikes above a certain threshold as pulses, we measured the pulse counts as a function of radiation dose from fully open to 99.96% shielding of the ^{137}Cs source. Fig. 4 gives the mmW pulse counts as a function of radiation dose measured at 0.75 m from the ^{137}Cs source. The log-log plot shows that the number of pulse counts increases linearly with the dose level, indicating a sensitivity level of 5 mR/h.

From the experimental data, we have calculated three parameters for the nuclear radiation-induced spark gap air breakdown: a) dependence of breakdown voltages on radiation dose, b) the spikes per second, and c) the mean and standard deviation of spike intervals. Fig. 5 shows the calculated parameters: (a) the breakdown voltage E_b versus dose on a logarithmic scale; (b) the breakdown spikes per second and its linear fitting to the Poisson statistics as given in (3); and (c) the measured mean time interval of breakdown spikes and its standard deviation. From Fig. 5(a), the reduction of breakdown voltage is up to 0.4 kV, which corresponds to a reduction of ~10% compared to normal air breakdown voltage. To compare it with respect to the reported values in the literature, a ~20% reduction is indicated for 150-KeV-X-ray pre-ionization of a graphite-steel

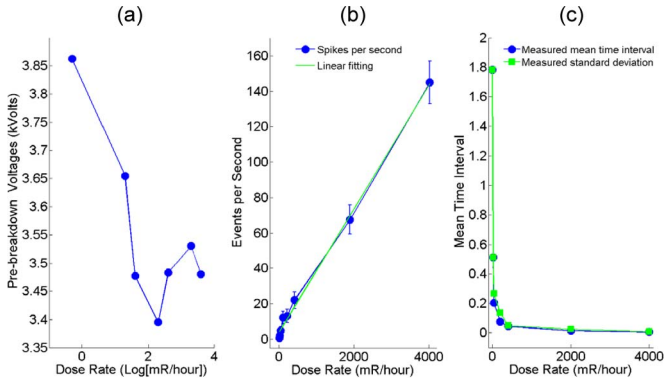

Fig. 5. Experimental and theoretical results: (a) measured breakdown voltage E_b, (b) number of breakdown spikes per second and its linear fitting, and (c) mean time interval between events and its theoretical Poisson standard deviation.

spark gap [17] and a ~50% reduction for the laser induced pre-ionization microwave methane/air mixture breakdown [18]. Two factors may contribute to the deviation of these values: 1) statistical process and 2) the inaccuracy in the readout of the power supply voltage during its relatively fast sweep (250 V/s). The random sequence of spikes is due to the random property of the nuclear radiation-induced free electrons, which follows the Poisson distribution. In terms of time interval between adjacent spikes τ, the probability distribution function is given by

$$P(\tau, \lambda) = \lambda \exp(-\lambda\tau) \tag{3}$$

where λ is the average spikes per second, which is the inverse of the average arrival time, i.e., $\lambda = 1/\overline{\tau}$; the standard deviation is $\sqrt{\overline{(\tau - \overline{\tau})^2}} = \overline{\tau}$. The average arrival time is inversely proportional to the ionized electrons per second or the nuclear radiation dose $\Re$, i.e., $\overline{\tau} \propto 1/\Re$, which yields the average spikes per second of $\lambda \propto \Re$. In Fig. 5(b), we linearly fitted the spikes per second to obtain the interaction volume of the spark gap, which gives the value of ~ 0.06 mm^3, or an effective length of ~0.2 mm, about 1/3 of the spark gap length of 0.635 mm. From Fig. 5(c), we can see that the values of the measured mean time interval and standard deviation closely follow the Poisson process.

The dependence of the diffusion coefficient on nuclear radiation at the breakdown electric field strength E_b, i.e., $D(\Re)$ can be obtained by expressing the ionization rate in terms of E_b [19], [20]

$$D(\Re) \sim \Lambda_{eff}^2 (3.9 \times 10^{-19} E_b^{5.33} - 6.4 \times 10^4)\ (\text{cm}^2/\text{s}). \tag{4}$$

The free electron diffusion constant without exposure to any nuclear radiation is given by $D(\Re = 0) \sim 943$ cm^2/second [3], [21], [22], from which we obtain the effective diffusion length

$$\Lambda_{eff} \sim 0.37 \text{ mm} \sim \frac{d}{2} \tag{5}$$

and the diffusion constant $D(\Re)$ from (4) in the presence of high nuclear radiation reduces to

$$D(\Re) \sim 5.3 \times 10^{-22} E_b^{5.33} - 88.5\ (\text{cm}^2/\text{s}). \tag{6}$$

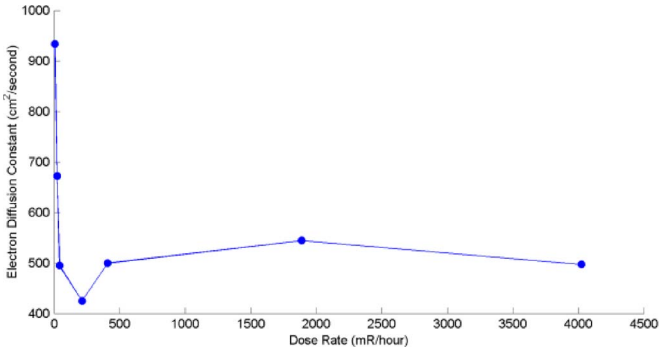

Fig. 6. Diffusion constant $D(\Re)$ for various nuclear radiation dose levels derived from experimental data according to (6).

Fig. 6 shows the diffusion constant $D(\Re)$ as a function of radiation dose, which shows a marked decrease in diffusion constant at high dose levels; for example, the diffusion constant is $\sim 500\ \mathrm{cm}^2/\mathrm{s}$ at 4000 mR/h, which is about 50% of the value $(\sim 1000\ \mathrm{cm}^2/\mathrm{s})$ at 5 mR/h.

V. Conclusion

We investigated the nuclear radiation-induced spark gap breakdown experimentally for various dose levels from 4000 mR/h to 5 mR/h. A mmW standoff system was used to monitor the breakdown in air. A log-log plot of the mmW pulse counts versus the radiation dose shows a linear change with a minimum detectable dose of 5 mR/h. It was observed that the breakdown electric field strength decreases with increasing dose level. We attribute it to the transition from the free electron diffusion when the dose is low to space charge-controlled diffusion when dose is high. The dependence of the diffusion constant on dose level was obtained from the experimental data, which shows that diffusion constant at high dose can be as small as 50% of the free electron diffusion constant. It was further observed that the mmW signal and the gap voltage traces exhibit a random spike sequence that follows the Poisson statistics, which is ascribed to the Poisson process of the nuclear radiation-induced air ionization. These findings shed new light on the problem of remote sensing of nuclear radiation.

Acknowledgment

We wish to thank Ray Kucera of Argonne's ESQ division for help with the operation of the Cs-137 calibration facility.

References

[1] Y. Hidaka, E. M. Choi, I. Mastovsky, M. A. Sapiro, J. R. Sirigri, and R. J. Temkin, "Observation of large arrays of plasma filaments in air breakdown by 1.5-MW 110-GHz gyrotron pulses," *Phys. Rev. Lett.*, vol. 100, no. 3, pp. 035003-1–035003-4, Jan. 2008.

[2] V. L. Granatstein and G. S. Nusinovich, "Detecting excess ionizing radiation by electromagnetic breakdown of air," *J. Appl. Phys.*, vol. 108, no. 6, pp. 063304-1–063304-5, Sep. 2010.

[3] A. D. MacDonald, *Microwave Breakdown in Gases*. New York: Wiley, 1966.

[4] W. E. V. J. Davies, J. Dutton, F. M. Darris, and F. L. Jones, "Electrical breakdown of air at high voltages," *Nature*, vol. 205, no. 4976, pp. 1092–1093, Mar. 13, 1965.

[5] J. S. Townsend and S. P. MacCallum, "Electrical properties of neon," *Philosoph. Mag.*, vol. 6, no. 38, pp. 857–878, 1928.

[6] J. S. Townsend and S. P. MacCallum, "Ionization by collision in helium," *Philosoph. Mag.*, vol. 17, no. 113, pp. 678–698, 1934.

[7] A. E. D. Heylen, "Simultaneous application of townsend and streamer theory," *Nature*, vol. 188, no. 4752, p. 734, Nov. 26, 1960.

[8] Loeb and Meek, *The Mechanism of the Spark Discharge*. Stanford, CA: Stanford Univ. Press, 1940.

[9] A. T. Afa, "Comparative analysis of breakdown characteristics for small and long air gaps," *Eur. J. Sci. Res.*, vol. 45, no. 1, pp. 324–332, 2010.

[10] A. D. MacDonald, D. U. Gaskell, and H. N. Gitterman, "Microwave breakdown in air, oxygen, and nitrogen," *Phys. Rev.*, vol. 130, no. 5, pp. 1841–1850, Jun. 1963.

[11] H. W. Bandel and A. D. MacDonald, "Effect of preionization on microwave breakdown in Neon," *J. Appl. Phys.*, vol. 40, no. 11, pp. 4390–4394, Oct. 1969.

[12] J. A. Miles, S. F. Adams, C. A. Dejoseph, and A. C. Laber, "Laser REMPI triggering of an air spark gap with nanosecond jitter," in *Proc. IEEE Int. Power Mod. High Voltage Conf.*, Las Vegas, NV, 2008.

[13] M. A. Gusinow and R. A. Gerber, "Space-charge-controlled diffusion in an afterglow," *Phys. Rev. A*, vol. 5, no. 4, pp. 1802–1806, Apr. 1972.

[14] R. A. Gerber and J. B. Gerardo, "Ambipolar-to-free diffusion: The temporal behavior of the electrons and ions," *Phys. Rev. A*, vol. 7, no. 2, pp. 781–790, Feb. 1973.

[15] I. D. Kaganovich, B. N. Ramamurthi, and D. J. Economou, "Spatiotemporal dynamics of charged species in the afterglow of plasmas containing negative ions," *Phys. Rev. E*, vol. 64, no. 3, pp. 036402-1–036402-12, Sep. 2001.

[16] L. Couedel, A. Mezeghrance, A. A. Samarian, M. Mikihian, Y. Tessier, M. Cavarroc, and L. Boufendi, "Complex plasma afterglow," *Contrib. Plasma Phys.*, vol. 49, no. 4/5, pp. 235–259, Jun. 2009.

[17] M. W. Ingram, "X-ray preionization for triggering spark gaps," M.S. thesis, Texas Tech Univ., Lubbock, TX, 1986.

[18] J. B. Michael, A. Dogariu, M. N. Shneider, and R. B. Miles, "Subcritical microwave coupling to femtosecond and picosecond laser ionization for localized, multipoint ignition of methane/air mixtures," *J. Appl. Phys.*, vol. 108, no. 9, pp. 093308-1–093308-10, Nov. 2010.

[19] J. T. Mayhan, "Comparison of various microwave breakdown prediction models," *J. Appl. Phys.*, vol. 42, no. 13, Dec. 1971.

[20] U. Jordan, D. Anderson, L. Lapierre, M. Lisak, T. Olsson, J. Puech, V. E. Semenov, J. Sombrin, and T. Tomala, "On the effective diffusion length for microwave breakdown," *IEEE Trans. Plasma Sci.*, vol. 34, no. 2, Apr. 2006.

[21] L. G. Huxley and R. W. Crompton, *The Diffusion and Drift of Electrons in Gases*. New York: Wiley, 1974.

[22] W. C. Taylor, W. E. Scharfman, and T. Morita, *Advances in Microwaves*, vol. 7. New York: Academic Press, 1971.

Shaolin Liao received the B.S. degree in materials science and engineering from Tsinghua University, Beijing, China, in July 2000, the M.S. degree in material science and the M.S. degree in electrical and computer engineering, both from the University of Wisconsin at Madison, in August 2003 and December 2005, respectively, and the Ph.D. degree in electrical and computer engineering from the University of Wisconsin at Madison, in May 2008. He held the Research Fellow Position in Physics Department, Queens College, City University of New York, New York City, from May 2008 to January 2010.

He is currently with Argonne National Laboratory, doing microwave/millimeter-wave/THz wave/laser research. He has been interested in both active and passive millimeter-wave applications like remote sensing, nondestructive examination and national security, both experiment and theory; high-power microwave transmission and conversion; gyrotron component design; microwave beam shaping technique; theory and algorithm development for high-performance simulation of electromagnetic wave propagation and scattering; antenna design and simulation; as well as microwave and light multiple scattering and Anderson localization inside random media.

Nachappa "Sami" Gopalsami (SM'95) received the B.E. and M.S. degrees in electrical engineering from the University of Madras, Chennai, India, and Ph.D. degree in electrical engineering and computer science from the University of Illinois, Chicago.

He joined Argonne National Laboratory in 1980 where he is currently a Senior Electrical Engineer in the Sensors and Instrumentation section of the Nuclear Engineering Division. He has published over 150 technical papers in the area of sensors and nondestructive examination and has seven U.S. patents to his credit. His current research interests include development of radio frequency, microwave, millimeter-wave, and terahertz sensors and imaging systems for national security, biosensing, environmental monitoring, and materials applications.

Dr. Gopalsami has received two R&D 100 awards from the R&D Magazine, both on millimeter-wave sensors in 1986 and 2007; an outstanding paper award from the American Society of Nondestructive Testing; and an Outstanding Mentor award from the Office of Science Undergraduate Research Programs. He is a senior member of IEEE and a member of Sigma Xi and SPIE.

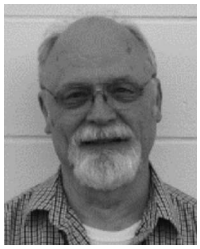

Eugene R. Koehl received the B.A. degree in physics from Lewis University, Romeoville, IL, in 1969, and the B.S. degree in electrical engineering from Midwest College of Engineering, Illinois Institute of Technology, Chicago, in 1981.

He is an Electrical Engineer at Argonne National Laboratory with 37 years of experience in the design, fabrication, instrumentation, control, and automated data acquisition of experiments and facilities for testing the design and characteristics of sensors, power systems and liquid metal reactor (LMR) components. His activities cover a broad range of physical sciences including acoustic signal transport, X-ray inspection and detection, high and process vacuum, alkali metal chemistry and heat transport, satellite tracking, and millimeter-wave systems. He has been involved with the precision manipulation and nondestructive testing of engineered materials used in heavy vehicle, stationary power, and aerospace systems for the past 16 years.

Thomas W. Elmer, II (M'07) received the B.S. degree in physics with minors in math and computer science from La Sierra University, Riverside, CA, in 1998 and the M.S. degree in physics from the University of Illinois, Chicago, in 2004.

While at La Sierra, he worked for the physics department, writing, and maintaining programs to run laboratory experiments. He has also lectured on Astronomy and Gravitational Physics for the department. In 1999, he joined Argonne National Laboratory as a student intern, eventually staying as a Software Engineering Associate for the System Technologies and Diagnostics Department of the Nuclear Engineering Division. He writes programming for modeling, motion control, data acquisition, and data analysis in the microwave, millimeter-wave, and terahertz sensors labs. In 2007, he received an R&D 100 award from R&D Magazine.

Alexander Heifetz received the Ph.D. degree in electrical engineering, M.S. degrees in physics, and B.S. degree (Summa Cum Laude) in applied mathematics, all from Northwestern University, Evanston, IL.

He is an Electrical Engineer with Nuclear Engineering Division at Argonne National Laboratory. He came to Argonne as Director's Postdoctoral Fellow with Nuclear Engineering Division. He has published over 20 peer-reviewed papers in major scientific journals and has one provisional US Patent. His research interests are in simulations and modeling for electromagnetic engineering, nuclear engineering, signal processing, and controls.

Hual-Te Chien received the B.S. degree in aeronautical and astronautical engineering from the Tamkang University, New Taipei, Taiwan, and M.S. and Ph.D. degrees in aerospace engineering and engineering mechanics from the University of Cincinnati, Cincinnati, OH.

He is currently a Principal Mechanical Engineer at Argonne National Laboratory. He has 24 years of experience in the area of sensor and instrumentation, nondestructive evaluation and testing (NDE/T), and smart/intelligent materials and structures development. Recently, he has been working on developing photoacoustic, laser induced breakdown spectroscopy (LIBS), and millimeter spectroscope techniques for remote sensing and environmental monitoring. He has been author or coauthor of more than 60 publications and awarded seven U.S. patents.

Dr. Chien received two R&D 100 Awards in 1994 and 2011 and an Argonne's Pacesetter Award for excellence in achievement and performance in 1997.

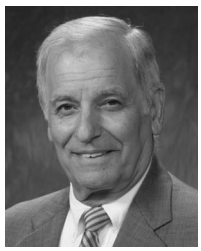

Apostolos C. Raptis (LM'06) is a Senior Electrical Engineer at Argonne National Laboratory (ANL) with 35 years of experience in teaching and in research and development. His areas of expertise include sensors, instrumentation and controls, nondestructive evaluation, data processing, electromagnetics, plasmas, optics, acoustics, and geophysical exploration. He is presently the Department Manager for Systems Technologies and Diagnostics in the Nuclear Engineering Division. At ANL, he initiated and helped develop ANL's instrumentation and nondestructive examination (I&NDE) programs for nuclear and fossil energy, conservation, and arms controls. He is responsible for work on national security for remote detection of chemical, biological, nuclear agents, and explosives. In addition, he has been a strong participant in collaborative work with the University of Chicago in the development of the Bioengineering initiative. He is the author of more than 250 publications and holder of 17 patents, as well as the recipient of the 1994, 1996, 2007, and 2011 R&D 100 awards, and 1994 ASNT best paper award.